Accelerometer Assisted Tracking for Free-Space Optical Communications

Shinhak Lee, James W. Alexander, Gerry G. Ortiz, and Chien-Chung Chen

Jet Propulsion Laboratory

California Institute of Technology

4800 Oak Grove Drive, Pasadena, CA 91109

Mailing address: 4800 Oak Grove Drive, MS 161/135, Pasadena, CA 91109, USA

Telephone: 818-354-3855, Fax: 818-393-6142, E-mail: Shinhak.Lee@jpl.nasa.gov

Abstract

We present a linear accelerometer based tracking concepts for free-space optical communications. A linear accelerometer is an attractive device since it is relatively small and inexpensive while the current technology has demonstrated its performance through several flight missions recently. Our traditional approach to optical communications pointing and tracking has been to rely solely on optical tracking with a few kilohertz update rate. Our study shows that by using an accurate linear accelerometer such as the AlliedSignal QA-3000, we could reduce the optical update rates needed from the focal plane array from few kilohertz to 30Hz. Double integration using the trapezoidal rule was used to estimate a displacement from accelerometer measurements and the associated errors were analyzed. Simulation results are derived using a QA-3000 accelerometer noise model. Experimental results are presented, which validate our analysis.

Subject terms: free-space optical communications; tracking; pointing; inertial sensor; accelerometer; double integration; line of sight stabilization.

1 Introduction

Accurate tracking of a ground receiver location and the pointing of downlink laser beam are critical functions required for the success of any free-space optical communications. This function has been known, in general, as the line of sight (LOS) stabilization to both space-based camera and optical pointing systems. Because of the tight pointing requirements, a spacecraft vibration, a major source of mis-pointing, needs to be compensated or suppressed during pointing downlink beam. Compensation for the spacecraft vibration requires fast position updates of the receiver. It has been reported that substantial compensation can be achieved by using a FPA capable of tracking at several kilohertz[4,5,6]. Currently, the typical method is to locate a receiver position through the detection of uplink beacon sources on focal plane arrays (FPAs) such as a CCD. The location of the beacon on the FPA can be directly translated into a pointing direction. Potential beacon sources include an uplink laser from ground telescope, extended sources (such as Earth and Moon), and star. Since the pointing accuracy is proportional to the rate at which the position of the beacon can be measured, the FPA should be read as fast as possible. The common drawback of these beacon sources, however, is that the light intensity is not usually sufficient to support the desired high update rate. One way to relax the fast update constraint is to combine optical tracking with inertial sensors. The role of inertial sensor is to measure high frequency spacecraft vibrations that cause jittery motion of beacon on FPA while optical tracking measures low frequency spacecraft vibrations. From the S/C vibration measurements, the beacon positions on FPA (hence the receiver position) can be estimated at a faster rate. In the past, similar approaches have been implemented where the combination of gyro and angular displacement sensors (ADS).[12] Other approach includes angular rate sensors instead of ADS.[13]

In this paper, we present the feasibility of using a linear accelerometer for tracking and pointing system of optical communications because of its small size, low mass, power and cost as well as the excellent performance demonstrated in recent flight missions.[8,9] The technique of using linear accelerometer pairs for measuring angular displacements also has the advantage that it can use the broad range of well developed linear accelerometer technologies while providing the vehicle's translatory accelerations[1]. The concept of accelerometer assisted tracking is depicted in Figure 1. In order to use linear accelerometer pairs to measure angular displacements, either software or hardware implementation is required to perform double integration. Previously, both hardware and software implementation for double integration were attempted. However, hardware implementation (analog double integration) was reported to have many significant problems whereas the proposed software implementation was limited to displacement signals with zero mean value due to the application of high pass filter.[10,11] Our motivation is to analyze the integration errors associated with the trapezoidal rule, a well-known numerical integration method without assuming any specific acceleration signal characteristics. Simulation and experimental results will be shown to validate the error analysis of the integration algorithm. Discussions on the minimum optical update rate for near Earth and deep space optical communications using accelerometer-assisted tracking will be presented.

2 Angle measurement using a pair of linear accelerometers

A pair of parallel mounted accelerometers A_1 and A_2 are shown in Figure 2. The angle, θ, can be estimated from the individual readings of accelerometers, A_1 and A_2, after converting the accelerations into linear displacements, d_1 and d_2 with the small angle assumption.

$$\theta = (d_1 - d_2)/ l \quad (1)$$

Since l, the separation, is a known measurable constant, θ is determined with the precision of A_1 and A_2. Angular displacements on two axis (α, β) can be obtained using three accelerometers as shown in Figure 3. Three accelerometers are placed on the y-z plane. Assume acceleration is in x-direction, then displacement estimation using accelerations from B and C gives an angular displacement (α) on x-y plane. Using A and the mean of B and C gives an angular displacement (β) on the x-z plane.

3 Position Estimation from Accelerometer Measurements

We assume that the spacecraft experiences the continuous acceleration represented as an acceleration function (a(t)). a(t) is sampled at a fixed rate, producing the samples denoted as a_N for its Nth sample, taken at time, T_N. The acceleration sample is assumed to require no integration time. The corresponding estimates for velocity and position are denoted as v_N and p_N, respectively. Let $a_N(t)$ represent continuous acceleration between sampled accelerations, a_N and a_{N+1}, where t=0 corresponds to the sampling time T_N. Since there is no further information available between two samples, we assume the intermediate acceleration value varies linearly. We introduce the linear interpolation function $a_N(t)$ with sampling interval of [0, Δt] defined by

$$a_N (t) = (a_{N+1} - a_N)t/ \Delta t + a_N \quad (2)$$

Note that for t =Δt,

$$a_N(\Delta t) = a_{N+1} \tag{3}$$

Let's consider only two sample points, a_N and a_{N+1}. The integration of a_N (t) from 0 to t gives the corresponding velocity v_N (t):

$$v_N(t) = (a_{N+1} - a_N)\, t^2/(2\Delta t) + a_N\, t + v_{N,}\ v_N \text{ the initial velocity at } t = 0 \tag{4}$$

For t =Δt,

$$v_N(t=\Delta t) = v_{N+1} = (a_{N+1} + a_N)\, \Delta t/2 + v_N \tag{5}$$

which is the area below the straight line connecting the two points, a_N and a_{N+1} (Figure 4). Notice that the error exists in velocity estimate due to the difference between the true area and our estimate because of our assumption on linearly varying acceleration. This velocity error propagates through position estimates. Similarly for position estimate,

$$p_N(t) = (a_{N+1} - a_N)\, t^3/(6\Delta t) + a_N\, t^2/2 + v_N\, t + p_{N,}\ p_N \text{ position at } t = 0 \tag{6}$$

For t =Δt,

$$p_N(t=\Delta t) = p_{N+1} = (a_{N+1} - a_N)\, \Delta t^2/6 + a_N\, \Delta t^2/2 + v_N\, \Delta t + p_N$$

$$= a_{N+1}\, \Delta t^2/6 + a_N\, \Delta t^2/3 + v_N\, \Delta t + p_N \tag{7}$$

The procedure in Eq. (6) can be summarized in Figure 5.

4 Error Analysis

Mainly two error sources, a random error and a frequency error cause the position estimation error. The random error is caused by accelerometer electronics (servo loop), data acquisition board, and signal conditioning unit. The frequency error is caused by non-uniform frequency response.

4.1 Random Error

In order to express the relationship between random error and position estimation error, Eq (6) needs to be rewritten in terms of acceleration with initial values of velocity and position. From Eq (6),

p_1, v_1 : initial values of position and velocity

$$p_2 = a_2 \Delta t^2/6 + a_1 \Delta t^2/3 + v_1 \Delta t + p_1$$

$$p_3 = a_3 \Delta t^2/6 + a_2 \Delta t^2/3 + v_2 \Delta t + p_2$$

$$= a_3 \Delta t^2/6 + a_2 \Delta t^2/3 + a_2 \Delta t^2/6 + a_1 \Delta t^2/3 + (a_2 + a_1) \Delta t^2/2 + 2v_1 \Delta t + p_1$$

$$p_4 = a_4 \Delta t^2/6 + a_3 \Delta t^2/3 + v_3 \Delta t + p_3$$

$$= a_4 \Delta t^2/6 + a_3 \Delta t^2/3 + a_3 \Delta t^2/6 + a_2 \Delta t^2/3 + (a_3 + a_2) \Delta t^2/2 +$$

$$a_2 \Delta t^2/6 + a_1 \Delta t^2/3 + (a_2 + a_1) \Delta t^2/2 + (a_2 + a_1) \Delta t^2/2 + 3v_1 \Delta t + p_1$$

$$\vdots$$

$$p_N = \Delta t^2(a_2 + \ldots + a_N)/6 + \Delta t^2(a_1 + \ldots + a_{N-1})/3 + (N-1)\, v_1 \Delta t + p_1 +$$

$$(N-2)a_1\Delta t^2/2 +$$

$$(2N-5)a_2\Delta t^2/2 +$$

$$(2N-7)a_3\Delta t^2/2 +$$

$$(2N-9)a_4\Delta t^2/2 + \ldots..$$

$$= \sum_{i=2}^{N-1} (N-i)a_i\Delta t^2 + (N/2-2/3)a_1\Delta t^2 + a_N\Delta t^2/6 + (N-1)\, v_1 \Delta t + p_1 \qquad (8)$$

where N is the number of acceleration measurements and Δt is the sampling period such that $N = T/\Delta t$ for the total integration time of T. As shown in Eq.(8), the knowledge of initial velocity (v_1) plays an important role in estimating the position. The equation indicates that the position estimation error is proportional to the error in initial velocity

and the integration period. Since the accelerometer does not provide initial velocity information, the initial velocity must be obtained either from direct measurements using lower bandwidth rate sensors such as gyros or from estimations using optical measurements of the beacon data. The effect of any error in initial velocity estimation will become larger as the integration period increases. The same is true for any acceleration bias present in acceleration measurements, which alters velocity. In this paper, we assume that there is no accelerometer bias and the initial velocity is known. Estimation of acceleration bias and initial velocity will be addressed in the next paper with implementation progresses.

The position estimation error (variance) can be expressed as a function of the random error (1 sigma value) in acceleration, σ_a, assuming the a_i's are iid (independent, identically distributed) random variables.

$$\sigma_{pN}^2 = (\Delta t^2)^2 \sum_{i=2}^{N-1} (N-i)^2 \sigma_a^2 + (\Delta t^2)^2 (N/2-2/3)^2 \sigma_a^2 + \sigma_a^2 (\Delta t^2)^2/6^2$$

The standard deviation of position estimation using N samples of acceleration measurements then becomes

$$\sigma_{pN} = \Delta t^2 \sigma_a \left(\sum_{i=2}^{N-1} (N-i)^2 + (N/2-2/3)^2 + 1/36 \right)^{1/2} \qquad (9)$$

The position estimation error (1 sigma value) for σ_a of 10μg and sampling rates of 2kHz, 5kHz, and 10kHz are plotted in Figure 6 for an integration period up to 100msec. An angular position estimation error can be derived from Eq.(1) assuming the two linear position estimates, d_1 and d_2 are iid random variables with its rms error of σ_{pN} in Eq.(9).

$$\sigma_\theta^2 = (\mathrm{Var}(d_1) + \mathrm{Var}(d_2))/l^2$$

$$= 2\,\sigma_{pN}^{\,2} / l^2$$

$$\text{or} \qquad \sigma_\theta = \text{sqrt}(2)\,\sigma_{pN} / l \qquad (10)$$

4.2 **Frequency Response Error**

This error is caused by the frequency response of the accelerometer servo loop. The maximum error for the frequency range of 0-300Hz is 0.5dB or 6% in magnitude for Alliedsignal QA-3000 accelerometer although the best performance delivered was 0.5% error. Since the angular displacement error is proportional to the acceleration error, the expected value of uncompensated angular platform jitter can be used to find the maximum allowable calibration error. Using Olympus S/C jitter model (S(f), Figure 7), for example, the uncompensated rms jitter can be estimated over frequency range of 10 to 300 Hz (Figure 7). In order to meet our error budget of 0.1μrad, for example, the calibration error should be better than 2.5% (4μrad * 2.5% = 0.1μrad). If the frequency range of up to 300 Hz is considered (uncompensated rms error of 16μrad), the calibration should be better than 0.6% which is within the current performance of QA-3000 accelerometers. Based on analysis and specifications, the current accelerometer (QA-3000) is accurate enough to compensate slow control loop, possibly, with up to 1 Hz update rate.

5 Simulation Results

5.1 Noise Modeling

The QA-3000 specifications show the following noise (1 sigma value, due to electronics, before signal conditioning and sampling) characteristics with scaling factor of 1.3158mA/g.[2]

The following procedures were used to generate QA-3000 noise characteristics for our simulations

a. Generate Gaussian noise
b. Compute PSD (Power Spectral Density)
c. Compute noise from PSD
d. Compare with QA-3000 specifications
e. Scaling of the noise to match QA-3000 specifications
f. Inverse FFT of PSD

As an example, Figure 9a and 9b shows the Gaussian noise and its PSD. Figure 9c and 9d show Gaussian noise and PSD after scaling in frequency domain. The results show that the noise in all frequency range (0-1kHz) has been reduced, particularly in the frequency range of (10-500Hz).

5.2 Estimation of linear displacements

Simulation results using the Gaussian noise in Figure 9 were computed from 50 runs and show the 1 sigma error in displacement estimation. The rms noises of the accelerations are 56μg and 39μg for 2kHz and 5kHz sampling, respectively. The simulation indicates that higher sampling frequency generally gives smaller displacement estimation error. Table 1 compares the simulation results with the analytical results (Figure 6) for various integration periods. Since the displacement estimation error is proportional to the rms noise (Eq. 9), the expected ratio based on 1 sigma noise is 5.6 for 2kHz (10μg vs. 56μg) and 3.9 for 5kHz sampling (10μg vs. 39μg). These results show that the ratio of 5kHz sampling results has better agreements with the analytical results.

6 Experimental Results

The laboratory setup consists of QA3000 accelerometer, signal conditioning unit and 16bit ADC. The measured acceleration noise include accelerometer electronics noise, signal conditioning unit noise, ADC quantization noise, and building vibrations. The measured noise showed 340μg (1 sigma value) from 20 runs for both 2kHz and 5kHz sampling. The measured acceleration noise samples were used to derive position estimation error and the results are shown in Figure 11. As was shown consistently in both analytical and simulation results (Figure 6 and 10), 5kHz results show smaller error than 2kHz sampling (Figure 11). The ratio of position estimation errors between the experimental results and the analytical results is again presented in Table 2. The expected error ratio based on 1 sigma noise is 34 (10μg vs. 340μg). The difference between analytical and experimental results is 10 to 20%, which is probably due to noise distribution different than the assumed perfect Gaussian distribution.

7 Discussion

The immediate benefit of accelerometer assisted tracking is the reduced requirement on FPA update rate. This outcome has a significant impact on the architecture of tracking and pointing subsystem of both near Earth and deep space optical communications. For beacon based near Earth missions, the beacon laser power can be reduced while the reduced requirement on FPA update rate opens the possibility of using commercial off the shelf cameras. For deep space missions, star tracker can provide the needed beacon update rate. Recent study showed that 10^{th} to 11^{th} magnitude stars could provide reference positions with the rate of 10 to 20Hz at arbitrary attitudes.[7]

For the proposed accelerometer assisted tracking, the key question is what the minimum FPA update can be assuming that the QA-3000 accelerometer is used in the tracking control loop. To provide an example we use the baseline design and accelerometer random error allocation for Europa mission study [3]. Assuming a separation of 30cm between two accelerometers, the resulting angle error (σ_θ) can be computed from Eq.10 as follows.

$$\sigma_\theta = 4.71\, \sigma_{pN} \qquad (11)$$

Derived from the allocated angle error of 0.071μrad (σ_θ), the linear displacement error, σ_{pN}, should not exceed 0.015μm. This corresponds to the FPA integration period 0.035seconds or equivalent FPA update rate of 30Hz (1/integration period) using simulation results of 5kHz sampling. This minimum FPA update rate is close to what star trackers can provide for deep space missions. Matching 20Hz of FPA update rate requires the error allocation be increased to 0.033μm (Figure 10).

The performance difference between simulation and experimental results is mainly from the fact that the laboratory measurements include building vibrations that can not be separated from other electronic noise. We believe that the low noise shown in simulation can be achieved in space, as was demonstrated in IPEX-I experiment where the minimum rms on-orbit disturbance was 84μg.[8]

8 Conclusion

We presented an accelerometer assisted optical communications tracking concept, algorithm, error analysis, simulation, and experimental results. The key performance parameter for tracking control using optical reference is the update rate of optical reference on the FPA. As one of the best linear accelerometers in the market,

AlliedSignal QA-3000 is promising to reduce the FPA update rate from several kilohertz to 30Hz. This concept can be implemented for the near Earth missions where the FPA update rate of several hundred hertz can easily be achieved using the uplink laser beacon. For deep space missions, inertial sensors combined with star tracker can provide the needed reference position updates to the tracking control loop.

Acknowledgement

The research in this report was carried out by the Jet Propulsion Laboratory, California Institute of Technology, under contract with the National Aeronautics and Space Administration.

References

1. Shmule Merhav, Aerospace Sensor Systems and Applications, Springer
2. AlliedSignal Aerospace, QA-3000 Accelerometer Data Sheet, 1994
3. C.-C. Chen, J. W. Alexander, H. Hemmati, S. Monacos, T. Y. Yan, S. Lee, J.R. Lesh, and S. Zingles, "System requirements for a deep-space optical transceiver", *Free-Space Laser Communication Technologies* XI, *Proc. SPIE*, Vol.3615, 1999.
4. M. Jeganathan, A. Portillo, C. S. Racho, S. Lee, D. M. Erickson, J. Depew, S. Monacos, and A. Biswas,"Lessons learned from the Optical Communications Demonstrator (OCD)", *Free-Space Laser Communication Technologies* XI, *Proc. SPIE*, Vol.3615, 1999.
5. Shinhak Lee, James W. Alexander, and Muthu Jeganathan, "Pointing and tracking subsystem design for optical communications link between the International Space Station and ground", *Free-Space Laser Communication Technologies XII, Proc. SPIE*, January, 2000.

6. H. Ansari, "Digital control design of a CCD-based tracking loop for Precision beam pointing", *Proceedings of SPIE OE/LASE'* 94, Vol. 2123, Los Angeles, CA, Jan. 1994.

7. J. W. Alexander, S. Lee, and C.-C. Chen, "Pointing and Tracking concepts for deep-space missions", *Free-Space Laser Communication Technologies* XI, *Proc. SPIE,*Vol.3615, 1999.

8. M. Levine, R. Bruno, and H. Gutierrez, "Interferometry program flight experiment #1: Objectives and Results", *Proceedings of 16th International Modal Analysis Conference*, Santa Barbara, California, 1998.

9. M. B. Levine, "On-Orbit Microdynamic Behavior of a Flexible Structure: IPEX II", *Proceedings of 17th International Modal Analysis Conference*, Kissimmee, Florida, 1999.

10. Ribeiro, J.G.T., Castro, J.T.P & Freire, J.L.F, "Problems in analogue double integration to determine displacemnents from acceleration data*", Proceedings of the 15th International Modal Analysis Conference*, pp.930-934, Orlando, Florida, 1997.

11. Ribeiro, J.G.T., Freire, J.J.F, and Castro, J.T.P, "Some comments on digital integration to measure displacements using accelerometers*", Proceedings of the 17th International Modal Analysis Conference*, pp.554-559, Orlando, Florida, 1999.

12. Michael F. Luniewicz, Jerold P. Gilmore, Tze Thong Chien, and James E. Negro, "Comparison of wide-band inertial line of sight stabilization reference mechanizations", *Proceedings of SPIE International Symposium on Aerospace/Defense Sensing*(Conference 1697) – *Acquisition, Tracking, and Pointing* VI, pp.378-398, 1992.

13. Dan Eckelkamp-Baker, Henry R. Sebesta, and Kevin burkhard, "Maghetohydrodynamic Inertial Reference System", *Acquisition, Tracking, and Pointing, Proceedings of SPIE*, Vol.4025, pp.99-110, 2000.

Table and Figure captions

Table 1. Error ratio between analytical and simulation results of displacement estimation.

Table 2. Error ratio between the experimental and the analytical results

Figure 1. Accelerometer assisted tracking concept

Figure 2. A linear accelerometer arranged to operate as an angular accelerometer

Figure 3. Triangular configuration of three accelerometers

Figure 4. Sampling of continuous acceleration a(t).

Figure 5. Diagram illustrating the position estimation procedure from acceleration measurements. Multipliers (c1 to c4) are: $c_1 = \Delta t$, $c_2 = \Delta t^2/3$, $c_3 = \Delta t^2/6$, $c_4 = \Delta t/2$.

Figure 6. Position estimation error vs. integration period. Acceleration measurement error of 10μg was used for two sampling frequencies (2kHz and 5kHz). Notice that higher sampling frequency gives better performance.

Figure 7. A frequency response error should be better than 2.5% for integration time of 0.1 second assuming an error budget of 0.1μrad given Olympus S/C base motion PSD.

Figure 8. Noise characteristics of QA-3000 accelerometer

Figure 9. (a), (b): simulated Gaussian noise (g) for 2kHz sampling and its PSD, (c), (d): simulated Gaussian noise (g) for 2kHz sampling and its PSD after scaling in PSD to satisfy QA-3000 noise specifications

Figure 10. Displacement estimation error (m) for two sampling frequencies (2kHz, 5kHz) given simulated QA-3000 accelerometer noise characteristics.

Figure 11. Displacement estimation error (m) for sampling frequency of 2kHz and 5kHz from Lab. measurements.

Table 1.

Integration period(sec) / Sampling freq.	0.02	0.04	0.06	0.08	0.10
2kHz	3.3	3.5	3.7	4.0	4.0
5kHz	3.6	3.6	3.7	3.6	3.6

Table 2

Integration period(sec) / Sampling freq.	0.01	0.02	0.03	0.04	0.05
2kHz	31	37	42	43	41
5kHz	41	45	46	44	40

Figure 1

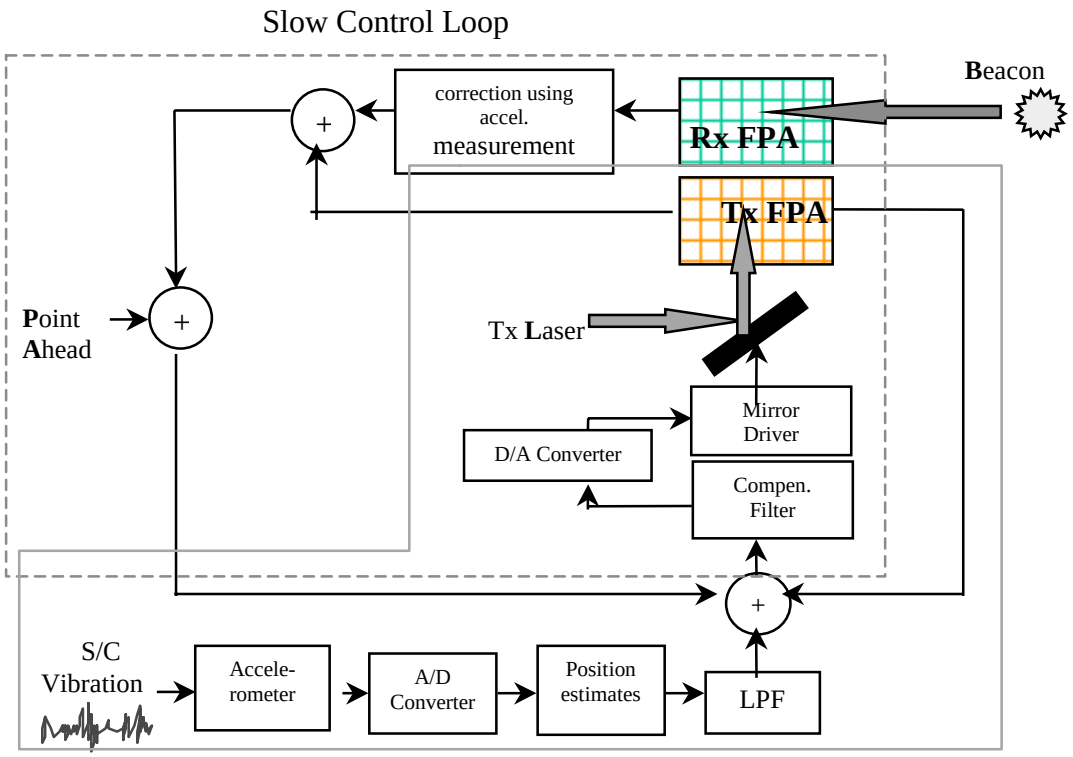
Slow Control Loop
Beacon
correction using accel. measurement
Rx FPA
Tx FPA
Point Ahead
Tx Laser
Mirror Driver
D/A Converter
Compen. Filter
S/C Vibration
Accele-rometer
A/D Converter
Position estimates
LPF
Fast control loop

Figure 2

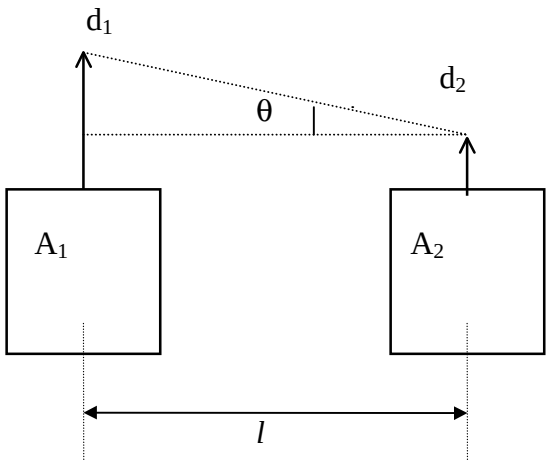

Figure 3

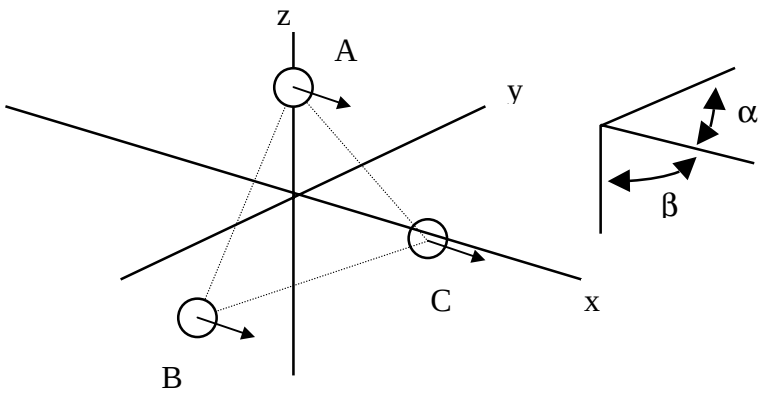

Figure 4

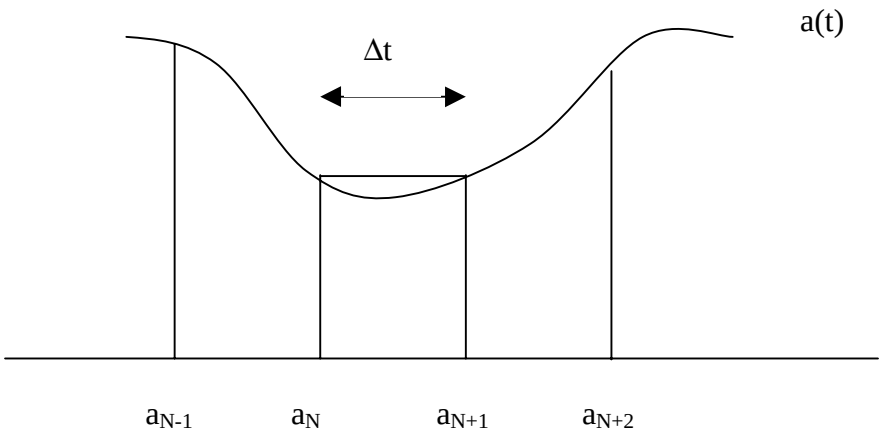

Figure 5

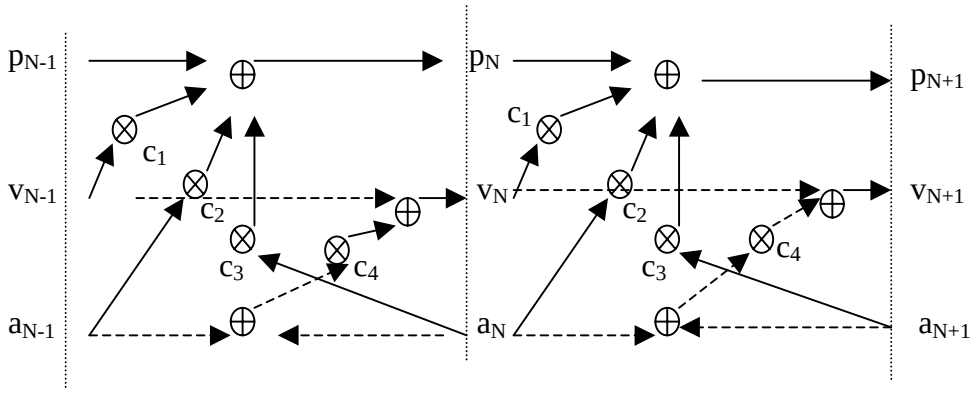

Figure 6

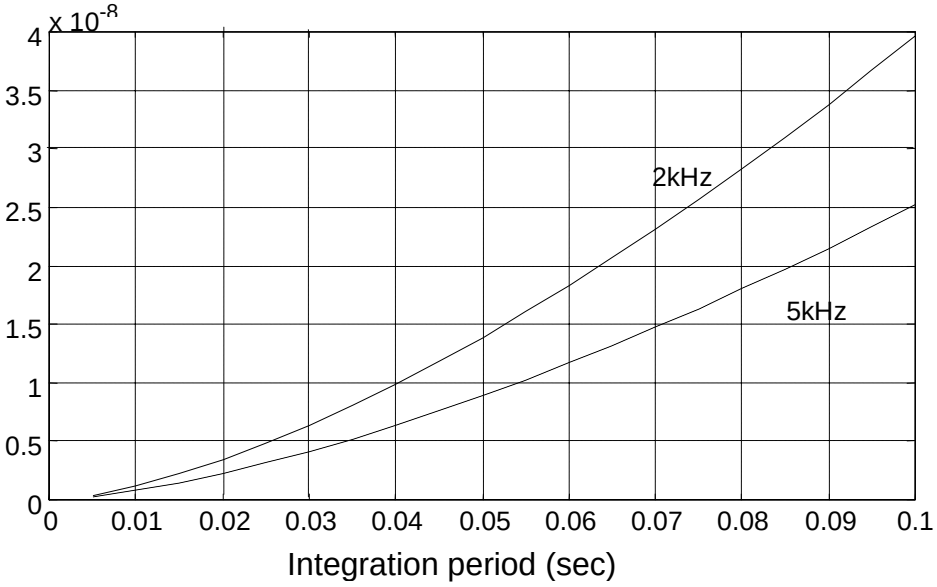
x 10^-8
4
3.5
3
2.5
2
1.5
1
0.5
0
0
0.01
0.02
0.03
0.04
0.05
0.06
0.07
0.08
0.09
0.1
2kHz
5kHz
Integration period (sec)

Figure 7

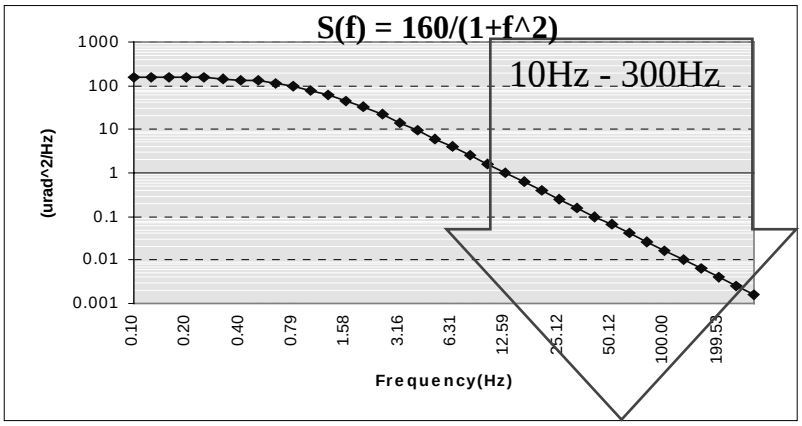

rms jitter of 4urad

Figure 8

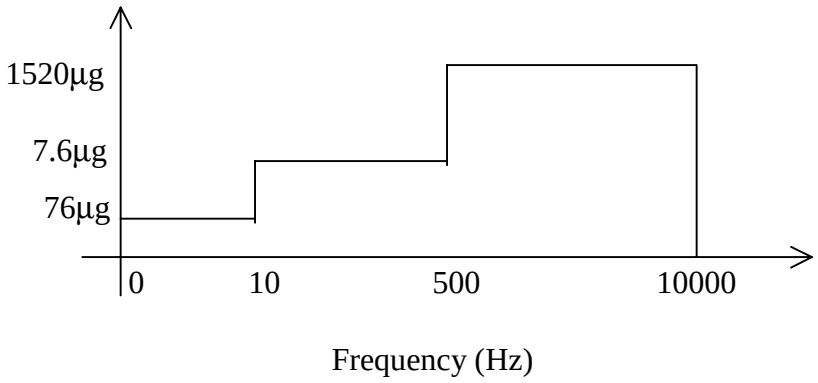

Figure 9

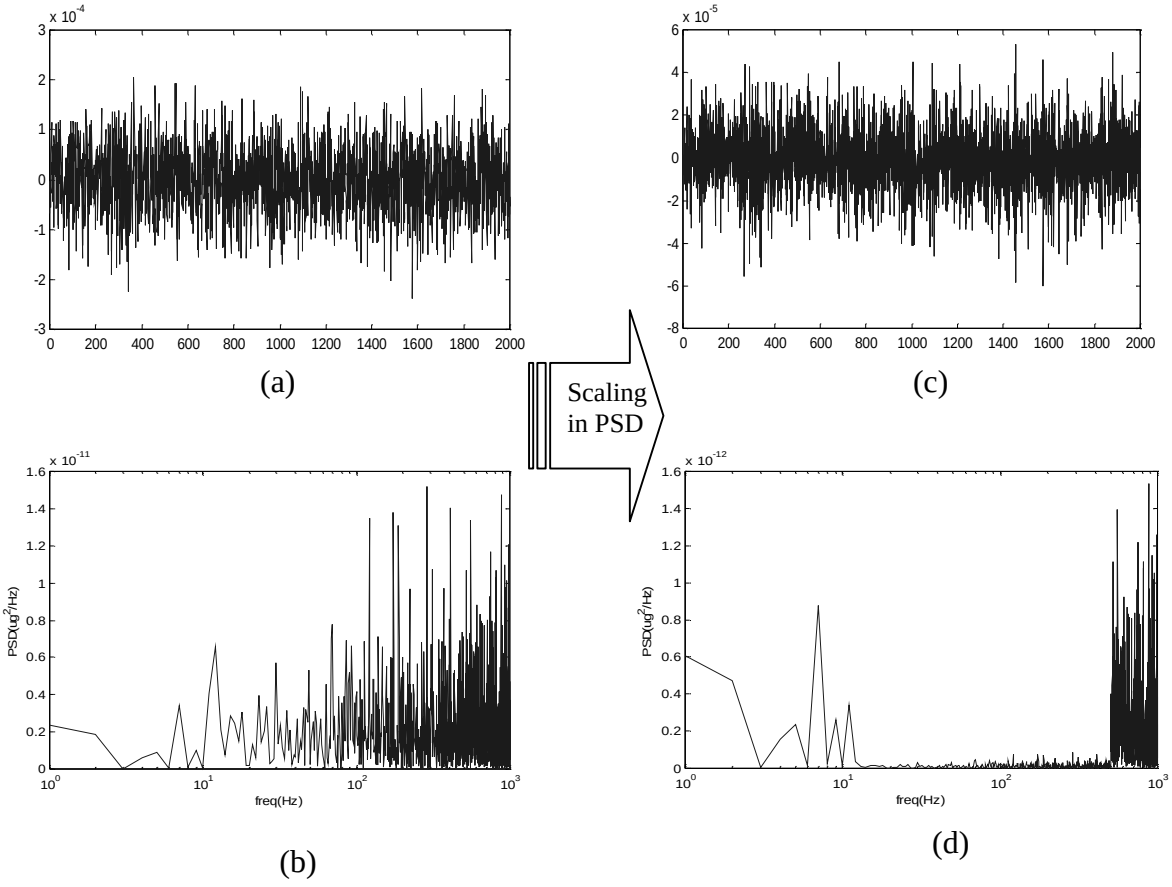
x 10^-4
(a)
x 10^-5
(c)
Scaling
in PSD
x 10^-11
PSD(ug^2/Hz)
freq(Hz)
(b)
x 10^-12
PSD(ug^2/Hz)
freq(Hz)
(d)

Figure 10

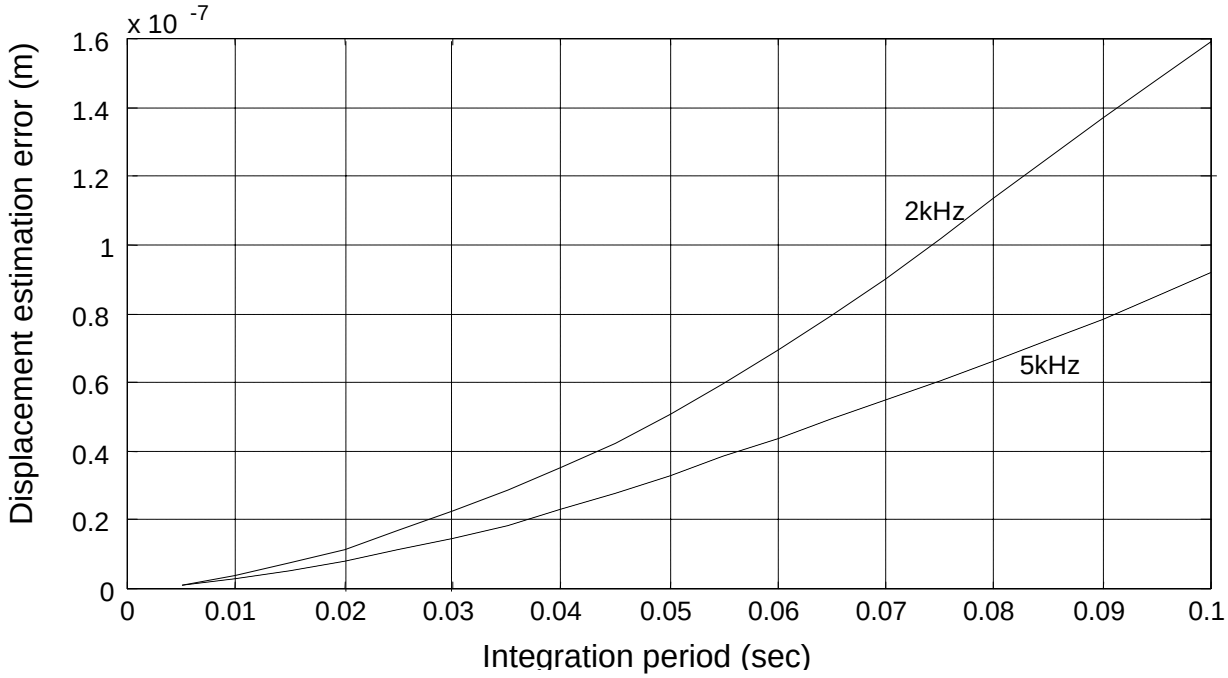
x 10 -7
Displacement estimation error (m)
1.6
1.4
1.2
1
0.8
0.6
0.4
0.2
0
0
0.01
0.02
0.03
0.04
0.05
0.06
0.07
0.08
0.09
0.1
Integration period (sec)
2kHz
5kHz

Figure 11

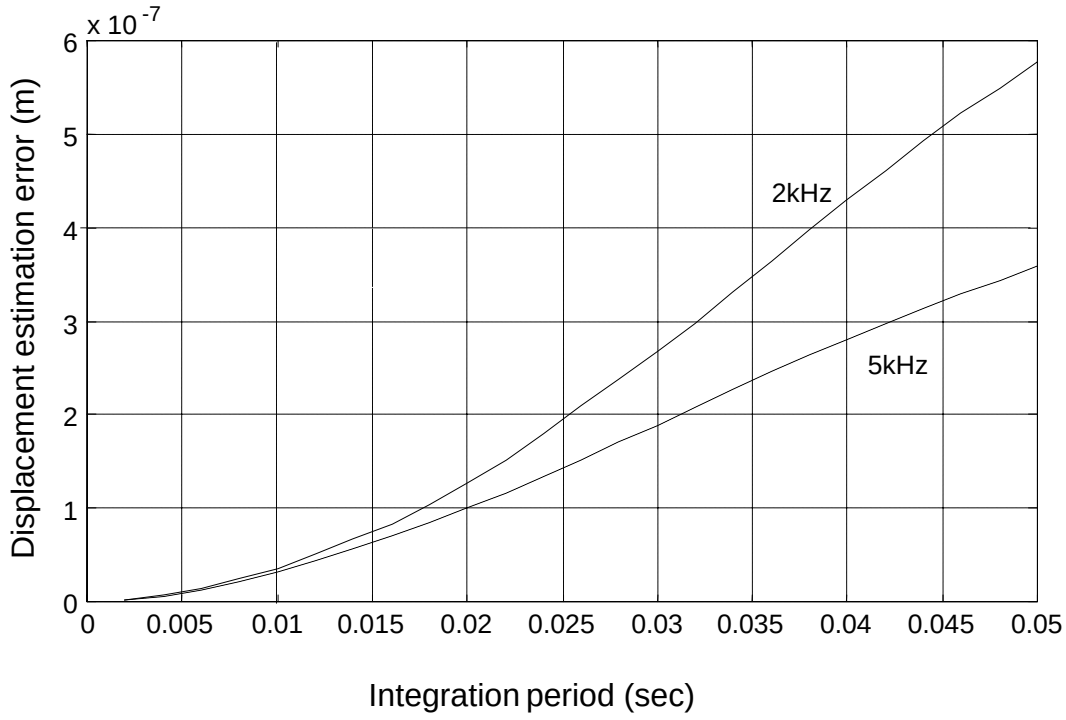
x 10 -7
6
5
4
3
2
1
0
Displacement estimation error (m)
2kHz
5kHz
0
0.005
0.01
0.015
0.02
0.025
0.03
0.035
0.04
0.045
0.05
Integration period (sec)